Polymer Chemistry

ROYAL SOCIETY OF CHEMISTRY

PAPER

View Article Online
View Journal | View Issue

Open Access Article. Published on 24 May 2024. Downloaded on 2/14/2026 11:39:17 PM.
This article is licensed under a Creative Commons Attribution-NonCommercial 3.0 Unported Licence.

Check for updates

Cite this: *Polym. Chem.*, 2024, **15**, 2362

Improved thermoset materials derived from biobased terpene macromolecules *via* photo-crosslinking†

Dimitrios Skoulas, [a] Fernando Bravo [a] and Arjan W. Kleij *[a,b]

Received 8th April 2024,
Accepted 7th May 2024

DOI: 10.1039/d4py00381k

rsc.li/polymers

A series of cross-linked materials was prepared *via* photo-induced reactions involving olefin-containing precursors and dithiols. The resultant materials (**M1–M6**) combine conventional feedstock with biobased ones and allow to forge hybrid thermosets whose properties were investigated by a range of analytical methods. Materials **M1** and **M2** served as references to compare with the biohybrid ones (**M3–M6**), whose thermal, spectra and mechanical properties can be easily regulated by the type of bio-component added to the overall composition. The biobased compositions allowed to expand the range of thermal properties and the degree of stiffness as measured by TGA, DSC and DMA, with the overall material morphology not being significantly altered as evidenced by SEM.

Novel materials that are able to combat the negative side-effects of climate change and shortage of petroleum-based resources contribute to a more sustainable future. In parallel, if such materials can be forged with improved and more modular properties, and with significantly reduced carbon footprints compared to purely fossil-fuel derived ones, they will undoubtedly create a vast interest from both academic and industrial laboratories.[1–4]

One of the most promising strategies towards the establishment of new materials is the construction of novel plastics with improved and/or expanded properties. Plastic materials combine a plethora of features that render them of great use in every-day life and in industrial applications. Furthermore, they exhibit advanced material properties and can be easily formulated, while they are typically cheap to manufacture. Depending on their composition and behavior, they are categorized into two main groups *viz*. thermoplastics, which can be reprocessed again, and thermosets which cannot.[5] Current and future efforts to produce better plastics are inspired by practices that lead to a circular use of macromolecules.[6,7] Additionally, a lower dependence on petroleum-based chemicals can favorably affect the overall carbon footprint of polymeric materials.[8]

In this respect, biomass-based raw materials have shown to act as feedstock for the preparation of polymers that can (partially) replace or reduce the utilization of the traditional petroleum-based polymers highlighting an important breakthrough in the field of sustainable chemistry.[9] Cross-linked polymers, that combine the advantages of thermoset and thermoplastic polymers while originating from renewable sources, have sparked increasing scientific interest surrounding their potential applications.[10] Biobased polymers can be categorized mainly into two groups being either natural polymers or synthetic ones.[11] Cellulose, lignin, starch are the most prominent examples of the first group, while synthetic biobased polymers can be derived from biobased precursors such as plant oils and amino acids.

One particular class of structurally diverse biomass-derived, chemical compounds are terpenes. Their relative abundance in nature combined with their chemical functionality makes them attractive for the design of materials with tunable mechanical, optical and thermal properties. In addition, many of these terpenes feature double bond functionalities which are suitable for epoxidation thereby furnishing new types of epoxy monomers, which serve towards the preparation of biobased polymers.[12–16]

A prominent and well-studied example within the known family of terpene oxides is limonene oxide (LO), which can be copolymerized with CO_2 yielding poly(limonene carbonate)s (**PLC**) with high glass transitions.[17–20] The advantages of its bio-origin, high level of functionality and depolymerization potential of **PLC** explain the increased efforts in using this

[a]*Institute of Chemical Research of Catalonia (ICIQ-CERCA), Barcelona Institute of Science & Technology (BIST), Av. Països Catalans 16, 43007 – Tarragona, Spain. E-mail: akleij@iciq.es*
[b]*Catalan Institute of Research and Advanced Studies (ICREA), Pg. Lluís Companys 23, 08010 – Barcelona, Spain*

†Electronic supplementary information (ESI) available: Experimental details, characterization data for all materials, and copies of relevant spectra and chromatograms. See DOI: https://doi.org/10.1039/d4py00381k

This journal is © The Royal Society of Chemistry 2024

Open Access Article. Published on 24 May 2024. Downloaded on 2/14/2026 11:39:17 PM.
This article is licensed under a Creative Commons Attribution-NonCommercial 3.0 Unported Licence.

polymer for various applications.[21–23] Moreover, recently it was reported that the estimated cost for **PLC** production is similar to the production cost of the petroleum-based polystyrene adding further to its potential use beyond academia.[24]

Catalytic ring-opening copolymerization (ROCOP) of LO and carbon dioxide is the main method for the synthesis of **PLC**, while ring-opening polymerization (ROP) of its *trans*-cyclic carbonate is also feasible.[23,25–28] In the ROCOP route, CO_2 offers a an additional renewable C1 building block for the synthesis of **PLC** being both highly available and cheap. A crucial parameter for the successful polymerization of **PLC** is the presence of a suitable catalyst due to the sterically demanding nature of the terpene oxide monomers. Until now, only two effective catalysts have been reported in literature. In 2004, Coates reported Zn(II)BDI based catalysts that efficiently copolymerize LO and CO_2.[29] Further progress was achieved by our group when reporting the development of a binary Al(III) aminotriphenolate complex/PPNCl catalyst [PPNCl = bis(triphenylphosphine)iminium chloride], as high conversion of both stereoisomers of LO (*cis* and *trans*) could be achieved.[30,31]

The existence of pendent double bond in each monomeric unit of **PLC** offers a possibility for post-modification using thiol–ene click chemistry for cross-linking reactions changing the final properties of the material.[18,32,33] This underlines the use of **PLC** for preparing new types of materials. Further to this, Greiner *et al.* investigated materials resulting from blending **PLC** with commodity polymers in order to explore the possibility of new materials.[34] However, a broader study centered on the covalent incorporation of **PLC** into other petroleum- or plant-based materials would be useful in this respect.

Herein we present novel plastic materials based on the covalent incorporation of **PLC** within either petroleum-based or plant-based matrices without changing the application potential to create thermoset materials. We considered both divinylbenzene (**DVB**) and 1,7-octadiene as fossil-fuel feedstock (Scheme 1) as these have been frequently used as cross-linking agents and would a priory be suitable co-reagents for **PLC** (Scheme 1) thereby increasing the overall bio-content of such hybrid structures. Second, we also wished to evaluate combinations of **PLC** with either geraniol or limonene (having a plant-based origin) to forge materials with a higher degree of bio-content. To this end, we thus examined well-established radical-initiated copolymerization of both of these aforementioned substrate combinations in the presence of phenyl-bis(2,4,6-trimethylbenzoyl)phosphine oxide (BAPO) as photo-initiator with a constant 20 wt% of **PLC** in each of the resultant materials. The cured plastic materials (through thiol–ene chemistry except for the **DVB**-based materials) were examined by different analytical methods investigating their thermal and mechanical properties, and the results demonstrate that the properties of fossil-fuel commercial matrices can be improved and expanded. In parallel, we here also report novel bioplastics with plant-based feedstock that form rubber-like materials with superior mechanical and thermal properties compared to their parent materials.

Our overall objective is to exhibit the successful preparation of more sustainable bioplastics, in comparison with the 100% petroleum-based, existing ones. This emphasizes the potential of **PLC** to be used as an additive for the synthesis of cross-linked thermoset materials by covalent anchoring to existing fossil-fuel derived matrices. The combined advantageous features of **PLC**, being its bio-origin and chemical functionality (*cf.*, pendent double bonds), make it an attractive choice as an additive for new, sustainable polymer and material development. **DVB** and 1,7-octadiene were chosen as representative examples of petroleum-based feedstock, while limonene and geraniol were also examined due to their related chemical structure and functionality compared to **PLC** and being characteristic examples of plant-based monomers. The overall approach should open up new avenues for the use of **PLC** and other types of bio-polycarbonates towards the creation of more sustainable thermosets.

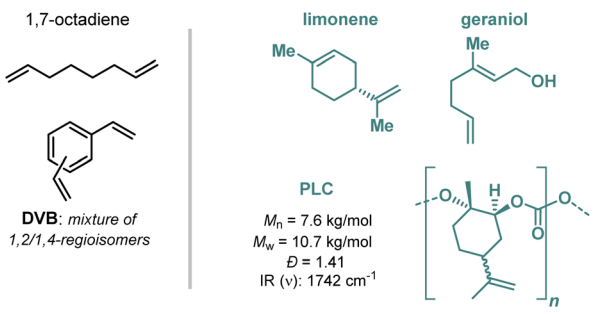

Scheme 1 Substrates used in this work to create cross-linked biobased matrices. **PLC** stands for poly(limonene carbonate), **DVB** is divinyl benzene.

Results and discussion

A standard procedure (see the Experimental section and ESI,† for details) for the cross-linking of all olefin-containing precursors and mixtures was used. As reference materials, cross-linked **DVB** and 1,7-octadiene (**M1** and **M2**, respectively) were prepared, while combinations of **DVB–PLC** (**M3**), 1,7-octadiene–**PLC** (**M4**), limonene–**PLC** (**M5**) and geraniol–**PLC** (**M6**) were also investigated (Scheme 2).

In order to prepare the different materials, all the components were mixed in a vial prior to their exposure to a lamp. The same preparation protocol was followed for all materials with the exception of **M1** and **M3**, that did not require a cross-linker (*i.e.*, ethane-1,2-dithiol) since it was possible to perform the cross-linking reaction without this additive. It is important to emphasize that in order to start the photo-initiated cross-linking, the overall reaction mixture needs to be homogeneous and **PLC** has to be fully dissolved into the mixture. In this respect, we found that a 20 wt% of **PLC** in the respective mixture was the highest possible amount to retain full homogeneity, as percentages such as 30% of **PLC** in all the studied matrices (see the ESI for details; Fig. S25–S28†) resulted in par-

Open Access Article. Published on 24 May 2024. Downloaded on 2/14/2026 11:39:17 PM.
This article is licensed under a Creative Commons Attribution-NonCommercial 3.0 Unported Licence.

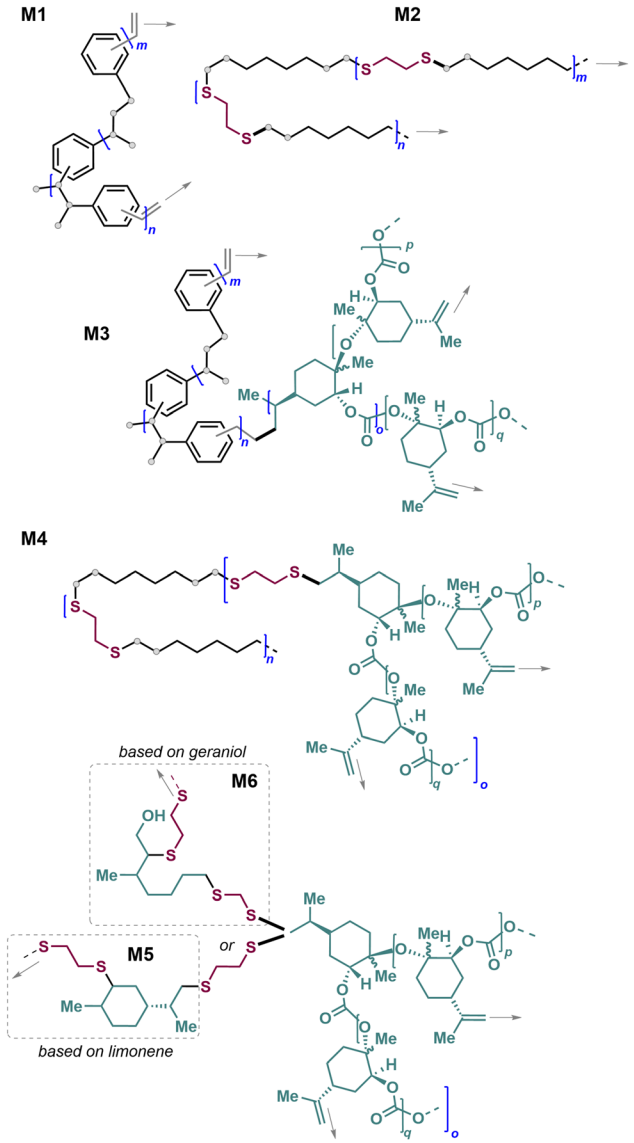

Scheme 2 Schematic structures of the materials **M1–M6** produced *via* direct or ethane-1,2-dithiol mediated photo-crosslinking.

tially heterogeneous/insoluble mixtures, likely leading to unpredictable and non-reproducible photo-polymerizations. Thus, we selected 20 wt% of **PLC** for the each of the envisioned materials to reach the highest possible bio-content within the final bio-composites.

The double bond functionalities present in **PLC** and the other starting materials offers the possibility for photo-induced, random radical polymerization with or without the presence of an appropriate crosslinker (ethane-1,2-dithiol), thereby leading to cross-linked materials **M1–M6**. The co-valently incorporation of **PLC** into the respective materials can be easily followed through IR spectroscopy (*vide infra*). BAPO was used as a reliable photo initiator since it undergoes homolytic α-cleavage at the carbonyl–phosphorus bond upon exposure to LED light at 405 nm [35,36] and it produces free-radicals with high efficiency, which promotes polymerization of vinyl monomers and double bond-containing compounds.[37]

Another challenge is the characterization of the final materials in terms of their structure. All the synthesized bioplastics are insoluble in the typical organic solvents, which limited the in-depth characterization of their structure by standard spectral and chromatographic techniques. Despite this general observation, the insoluble character of the obtained materials **M1–M6** offers as a possible advantage their exploitation in applications for which hydrophobic and/or insoluble materials are required such as in sealants or rubbers.

The cross-linking reactions were typically followed by IR spectroscopy as the absorption bands related to the double bonds of the involved substrates are highly diagnostic. Furthermore, in the hybrid materials with an increase bio-content (with **PLC**, limonene and/or geraniol), IR spectroscopy also allows to examine the stability of the polycarbonate as the linear carbonate group absorption typically falls in the region 1740–1760 cm^{-1}.[26,38,39]

Fig. 1 shows two representative cases involving the synthesis of cross-linked materials **M3** and **M4** containing a **DVB–PLC** and 1,7-octadiene–**PLC** combination, respectively. In Fig. 1a, a comparative IR spectral analysis between the parent **DVB** and **PLC**, and the hybrid cross-linked **M3** (**DVB–PLC**) shows that upon cross-linking the two components *via* photo-initiated radical addition, the main polycarbonate chain is unaffected as shown by a clear carbonate band at ν = 1744 cm^{-1} in the blue trace. Furthermore, the double bond absorption of the **PLC** around 1650 cm^{-1} (Fig. 1b, orange trace) for a larger part disappeared upon reaction, indicating a good-to-high level of C=C conversion. Both observations are in line with a successful cross-linking process.

The second case (Fig. 1c and d, **M4**) illustrates the cross-linking between 1,7-octadiene and **PLC**, with a clear presence of carbonate groups in the hybrid cross-linked material **M4** after photo-irradiation (Fig. 1c, absorption at 1744 cm^{-1}). In addition, C–H wagging peaks in the region 750–900 cm^{-1} can be found for parent **PLC** (Fig. 1d; orange trace), which after the cross-linking process are virtually lost. This is a strong indication that high C=C bond conversion in **PLC** had taken place.

Similar IR spectroscopic changes were observed for materials **M5** and **M6** (see the ESI† for details), and combined together it supports the overall efficacy of the used photo-induced cross-linking of various combinations of substrates with **PLC** to afford the partially biobased matrices **M1–M6** under user-friendly process conditions. It should be noted that the attempted cross-linking of limonene and geraniol in the absence of **PLC** as co-substrate led to materials with lower cross-linking degrees and typically required longer reaction times as evidenced by their physical appearance and IR analysis, thus pointing at a beneficial effect of adding **PLC** as a promoting cross-linking agent (see the ESI† for further details).

Next, we turned our attention to characterize the different materials using other techniques. First, photos of **M3–M6**

 This journal is © The Royal Society of Chemistry 2024

Open Access Article. Published on 24 May 2024. Downloaded on 2/14/2026 11:39:17 PM.
This article is licensed under a Creative Commons Attribution-NonCommercial 3.0 Unported Licence.

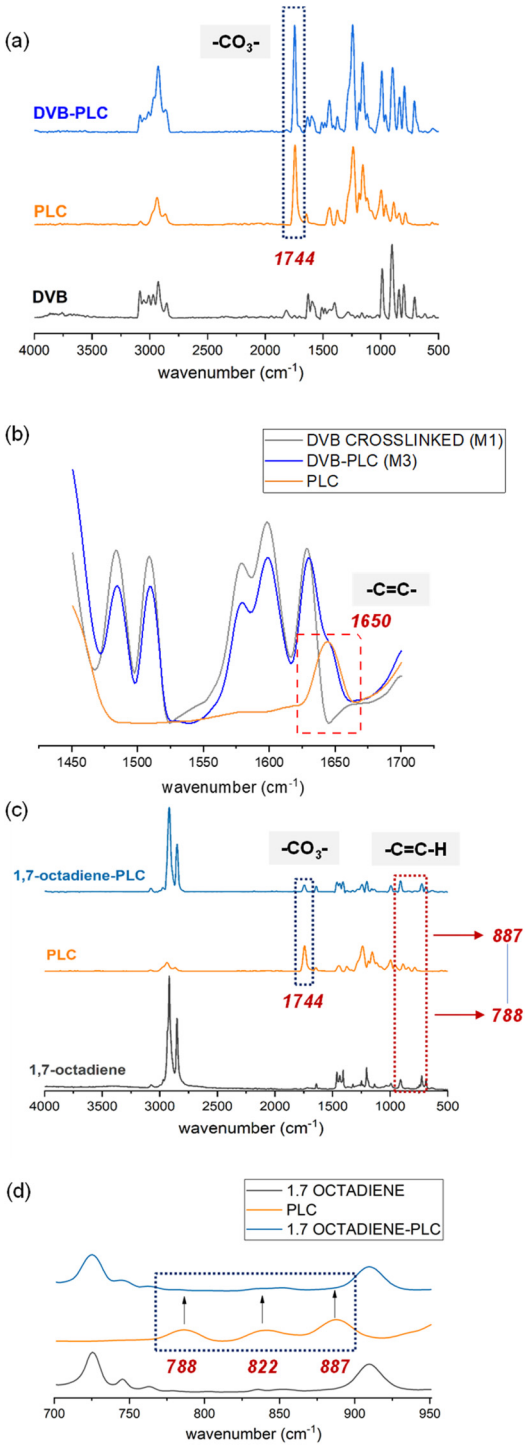

Fig. 1 (a) IR spectrum of cross-linked **M3** (**DVB–PLC**) and its comparison to the reference crosslinked materials **PLC** and **DVB**. (b) Selected expansion of the IR spectra for crosslinked **M3**, **PLC** and **DVB**. (c) IR spectrum of cross-linked **M4** (1,7-octadiene–**PLC**) and its comparison to the reference crosslinked materials **PLC** and 1,7-octadiene. (d) Selected expansion of the IR spectra for crosslinked **M4**, **PLC** and 1,7-octadiene.

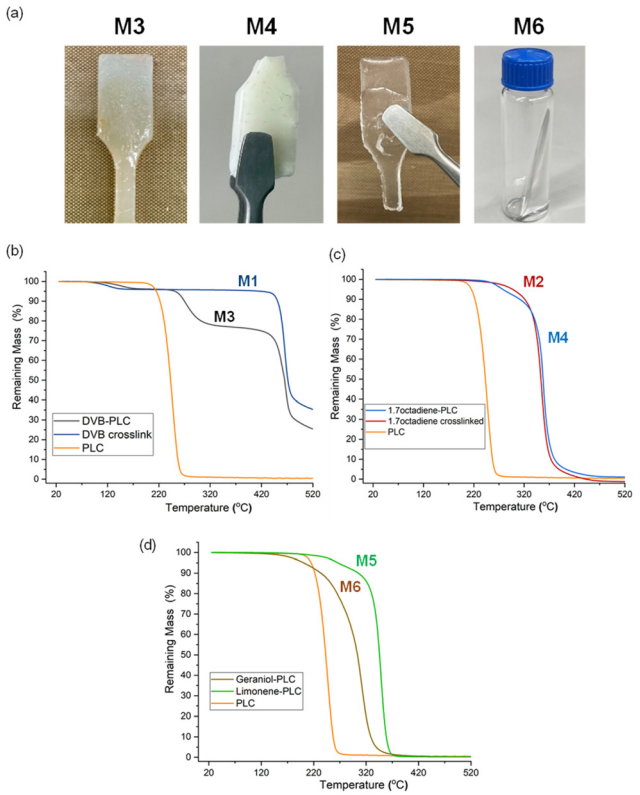

Fig. 2 Physical appearance of materials **M3–M6** (a) and their corresponding TGA analysis (b–d).

show the different textures that are obtained after photo-crosslinking (Fig. 2a). The hybrids **M3–M5** display solid materials with different degrees of flexibility and hardness (discussed further below), while **M6** represents a softer and more bendable material. Since the prepared solutions were transferred in a Teflon based mould, the final biomaterials obtained their shape after light exposure. However, **M6** was much softer, rubbery-like material (as indicated by DMA analysis, see Fig. S19 and S20 in the ESI†) and it was thus prepared inside the vial upon exposure to light. The other materials were processed in a complete "dog bone" shape (details in the ESI†). In order to investigate the influence of incorporating **PLC** into the cross-linked matrix, thermogravimetric analysis (TGA) was carried out for **M1–M6** (selected and typical examples for **M3** and **M4** are shown in Fig. 2b–d). It is clear that pristine **PLC** has the lowest thermal stability with an onset decomposition at around 200 °C (orange traces in Fig. 2b). An earlier thermal transition (>70 °C) present in cross-linked **DVB** is retained in the **DVB–PLC** hybrid, while two further transitions (not present in cross-linked **DVB**) occur at around 245 and 390 °C.

These data seem to indicate a higher stability of the cross-linked **PLC** in **M3** compared to the parent polymer. These transitions are not equally observed for **M4–M6** (Fig. 2c and d), and for **M4** a first onset is observed at 245 °C with a second one initiating at 330 °C. For **M5** and **M6**, a first onset decomposition starts around 120 °C but compared with the parent **PLC** (Fig. 2d, orange trace) the rate of decomposition is much slower and requires a higher temperature to proceed. Thus, these latter data indicate as well that the hybrid struc-

Open Access Article. Published on 24 May 2024. Downloaded on 2/14/2026 11:39:17 PM.
This article is licensed under a Creative Commons Attribution-NonCommercial 3.0 Unported Licence.

tures **M3–M6** show better overall thermal endurance than the polycarbonate **PLC** reference.

We also examined the materials **M1–M6** by differential scanning calorimetry (DSC, see Fig. 3 for selected examples and the ESI† for further details). In all cases studied, we observed typical melting points for the cross-linked, hybrid polymer samples. For **M4** (the 1,7-octadiene–**PLC** hybrid; Fig. 3a; data from the 3rd heating curve), the observed T_m was located at 79 °C, while for **M6** (geraniol–**PLC** hybrid; Fig. 3b), a T_m at 91 °C was observed. For **M3** based on **DVB** and **PLC**, an even higher and single T_m of 154 °C was detected (see the ESI†), while for **M5** (the limonene–**PLC** hybrid, ESI†), a T_m was noted at 133 °C. Additionally, for **M4** and **M5** a second peak at lower temperature was noted (49.8 °C and 73.3 °C, respectively), which could suggest a separate, second phase or an additional structural change occurring at higher temperature.

In order to gather information on the viscoelastic behavior of the newly prepared materials **M1–M6**, we carried out dynamic mechanical analysis (DMA). An example DMA result is provided in Fig. 4, for all other DMA results see the ESI† and Table 1. From a comparative analysis of the storage modulus E' measured for **M3** (**DVB–PLC** hybrid) and the parent **M1** (Table 1, entries 1 *vs.* 3), a clear and significant increase in the stiffness of the hybrid material can be noted (269.0 → 482.2 MPa), being an increase of nearly 80%. An even larger effect was detected for the hybrid **M4** (1,7-octadiene–**PLC**) compared to 1,7-octadiene itself (Table 1, entries 2 *vs.* 4),

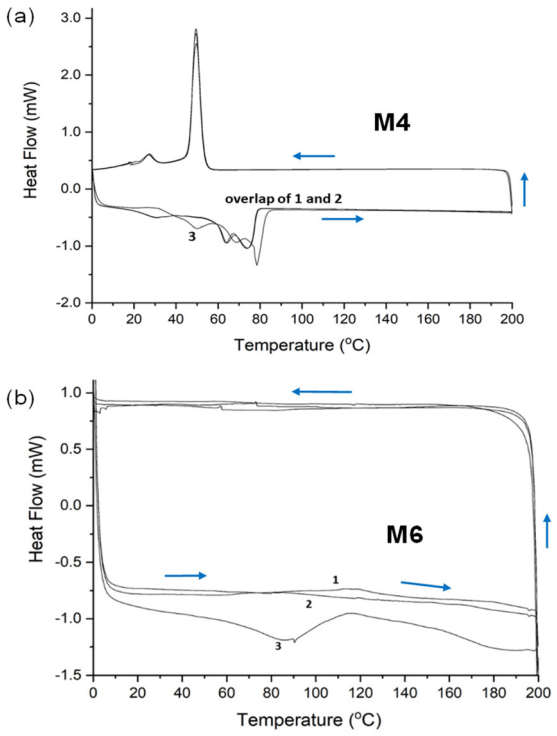

Fig. 3 (a and b) Selected DSC traces for materials **M4** and **M6**, respectively. The indices 1–3 refer to the consecutive heating curves in these DCS analyses.

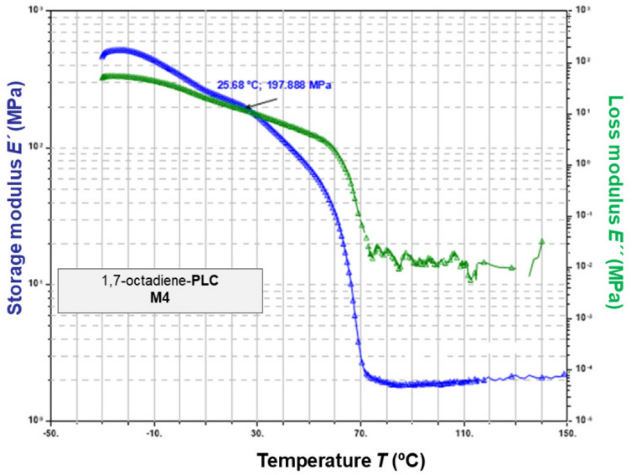

Fig. 4 DMA results for material **M4**.

showing an increase of the storage modulus from 84.2 to 200.8 MPa (a 138% increase).

For materials **M5** and **M6** based on combination of biocomponents **PLC** with limonene and geraniol, respectively, such comparisons were not feasible as the level of cross-linking did not provide materials useful for DMA analysis as evidenced by their physical inspection and IR spectroscopy (see the ESI†). For both **M5** and **M6** (Table 1, entries 5 and 6), the measured E' values were substantially lower than those collected for **M3** and **M4**, pointing at relatively flexible materials and indeed both were rubbery-like. The different relaxation processes in comparison to samples **M3** and **M4** indicates the high structural flexibility of the **PLC**/limonene-based material. Altogether, these different combinations of (bio)components with **PLC** allow to modulate the storage moduli over a wider range of values compared to their parent cross-linked materials, while introducing different degrees of bio-content of up to 68 wt%.

Additionally, it is important to stress the nature of the respective starting materials in relation to the properties of the final cross-linked materials, as these had markedly different mechanical properties despite adding the same amount of **PLC**. This agrees with the physical appearance of the final bio-hybrids, since **M2** and **M4** are opaque similar to **M1** and **M3**, showing the strong influence of their crosslinked matrix. A direct relative comparison involving **M5** and **M6** is impossible since limonene and geraniol themselves could not be obtained as crosslinked materials without the addition of **PLC**, emphasizing the importance of its presence in the final composition.

Further to this, DMA analysis offers the opportunity to gather insight information about the molecular weight between crosslinks (M_c) and the crosslinking density (CD), exploiting the obtained data of the storage modulus at the rubbery state.[40,41] A quantitative calculation of those parameters was processed for all the samples that had **PLC** cross-linked to the petroleum- or plant-based precursors (*i.e.*, **M3–M6**) to investigate its crosslinking density. For **M1** and **M2**, it

 This journal is © The Royal Society of Chemistry 2024

Open Access Article. Published on 24 May 2024. Downloaded on 2/14/2026 11:39:17 PM. This article is licensed under a Creative Commons Attribution-NonCommercial 3.0 Unported Licence.

Table 1 Summary of all data collected for materials **M1–M6**

M	Bio%[a] (wt%)	IR[b] (cm^{-1})	T_d^5 [c] (°C)	T_m [d] (°C)	T_g [e] (°C)	E' [e] (MPa)	M_c [f] (g mol^{-1})	CD[g] (mol cm^{-3})
M1	0	1630	419	149.3	122.5	269.0	—	—
M2	0	920, 1640	297	87	69.2	84.2	—	—
M3	13	1630, 1744	251	154.3	74.1	482.2	64	0.0166
M4	12	788, 822, 887, 920, 1640, 1745	277	49.8, 78.5	56.9	200.8	5184	0.0002
M5	65	1744	266	73.3, 133.3	−1.8	26.3	317	0.0034
M6	68	1744	201	90.5	−28.6	0.034	173 220	6.5×10^{-6}

[a] Calculated from the mass of each component introduced in the cross-linking experiment. Note that here no correction for the oxidation of the monomer LO in the case of **PLC**-based materials was applied. [b] Determined by IR spectroscopy (neat) providing the most diagnostic absorption bands. [c] Determined by TGA analysis, the T_d^5 stands for the decomposition temperature at 5 wt% loss. [d] Obtained from DSC analysis using the data from the 3rd heating curve. [e] Data extracted from the dynamic mechanical analysis (DMA) curves, see the ESI† for details. E' is the he storage modulus expressed in MPa at 25 °C. [f] Molecular weight between crosslinks (M_c). [g] Crosslinking density (CD) was calculated by dividing the polymer density by M_c.

was not possible to detect the plateau zone at the rubbery state. Comparison of the crosslinking densities between materials **M3** and **M4** (petroleum-based matrix) and **M5** and **M6** (plant-based matrix), can shed light on the relationship between this parameter with the viscoelastic behavior of the respective samples.

From Table 1 it is clear that material **M3** has the highest crosslinking density at the lowest molecular weight between the crosslinks. This seems to relate well with the storage modulus data, as **M3** also possesses the highest value among the series **M3–M6**. Comparatively, **M6** has both the lowest crosslinking density and the lowest storage modulus, while having the highest molecular weight between the crosslinks. The cyclic nature of **DVB** and limonene, and the different, linear structure of 1,7-octadiene and geraniol may be partially responsible for the noted differences in the series **M3–M6**.

Finally, we evaluated the overall morphology of the materials by scanning electron microscopy (SEM, Fig. 5). Selected SEM images are presented for the parent material **M1** and its co-cross-linked biohybrid **M3**. Judging from the representative images in Fig. 5, the overall crosslinked structures do not show significant changes when adding **PLC** as a component, which suggest that the use of **PLC** should not imply any practical objection when combined with typical fossil-fuel based substrates such as **DVB** and 1,7-octadiene (or others) to create new types of hybrid materials. Furthermore, the combination of **PLC** with the other biobased precursors upon crosslinking results into a uniformal surface of the final materials. Careful examination of the SEM photos shows no visible indication of porosity and a smooth surface area in the networks for all samples. In addition, the SEM photos reveal a homogenous network for all the samples **M1–M6** with and without the presence of **PLC**. The observation of dense polymer networks is made for all the samples independently of the presence of **PLC**.

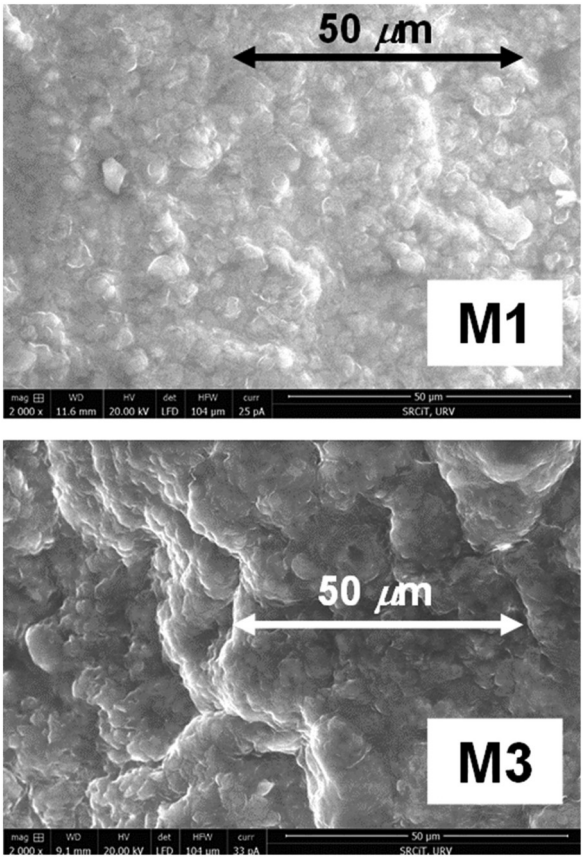

Fig. 5 Selected SEM images of the materials **M1** and **M3** with an inserted scale. For more details and images, see the ESI.†

Conclusions

In summary, we have prepared a family of new hybrid materials by using a practical and straightforward photo-crosslinking approach. The hybrid materials contain different degrees of biobased content (**PLC**, geraniol, limonene; 12–68%) and were analysed by a range of techniques with their data compared to the parent cross-linked materials where possible. From the data obtained, we conclude that the addition of **PLC** and its cross-linking proceeds with success and the storage modulus (E') can be markedly improved as shown in materials **M3** and **M4**. Biobased combinations of **PLC** with limonene and geraniol offer additional possibilities

Open Access Article. Published on 24 May 2024. Downloaded on 2/14/2026 11:39:17 PM. This article is licensed under a Creative Commons Attribution-NonCommercial 3.0 Unported Licence.

to access materials with a lower stiffness (rubbery-like), and higher degrees of overall bio-content. This work further demonstrates the potential of biobased polycarbonates such as **PLC**[42] as possible drop-in additives towards the creation of more sustainable thermoset materials.

Experimental section

Typical cross-linking experiment

0.80 g of substrate (**DVB** technical grade 80% Sigma-Aldrich; mixture of regio-isomers, 1,7-octadiene, limonene or geraniol) and 0.20 g of **PLC** were weighed into a screw-capped glass vial. Note that in the case of **DVB**-containing reaction mixtures, the cross-linking was done in the absence of ethane-1,2-dithiol, while in all other cases this cross-linking agent was added in stoichiometric amount with respect to the double bonds present (ratio 1 : 1). Then 0.010 g of BAPO was added following vigorous stirring, and the content of the vial was transferred in a Teflon based mould and a 405 nm (0.5 mW cm^{-2}) lamp was used to apply light over the mould. After 20 minutes, the final composite material was formed (**M3–M6**), and removed from the mould. **DVB** and 1,7-octadiene were also separately cross-linked for comparative reasons following the same protocol without adding **PLC**, providing as such cross-linked reference materials **M1** and **M2**.

Author contributions

DS carried out all the experiments and the analytical interpretation, AWK assisted DS during the project with feedback and scientific input, DS and AWK designed the project, while FB provided feedback on the results and wrote the manuscript in collaboration with DS and AWK.

Conflicts of interest

There are no conflicts to declare.

Acknowledgements

The authors thank the Cerca Program/Generalitat de Catalunya, ICREA, MINECO (PID2020-112684GB-100 and Severo Ochoa Excellence Accreditation 2020–2023 CEX2019-000925-S) and AGAUR (2021-SGR-00853) for support. This work has further received funding from the European Union's Horizon 2020 research and innovation programme under Marie Skłodowska-Curie grant agreement no. 801342 (Tecniospring INDUSTRY) and the Government of Catalonia's Agency for Business Competitiveness (ACCIÓ: COMBILOOP, ACE026/21/000087). We thank Prof. Silvia de la Flor from the Universitat Rovira i Virgili (Tarragona; Spain) for the DMA analyses and interpretation. The CTD unit of ICIQ is acknowledged for the TGA and DSC analyses.

Notes and references

1 M. Yang, L. Chen, J. Wang, G. Msigwa, A. I. Osman, S. Fawzy, D. W. Rooney and P. S. Yap, Circular economy strategies for combating climate change and other environmental issues, *Environ. Chem. Lett.*, 2023, **21**, 55–80.
2 L. Chen, L. Wang, D. W. Cho, D. C. W. Tsang, L. Tong, Y. Zhou, J. Yang, Q. Hu and C. S. Poon, Sustainable stabilization/solidification of municipal solid waste incinerator fly ash by incorporation of green materials, *J. Cleaner Prod.*, 2019, **222**, 335–343.
3 R. W. Bentley, Global oil and gas depletion: An overview, *Energy Policy*, 2002, **30**, 189–205.
4 G. Chyr and J. M. DeSimone, Review of high-performance sustainable polymers in additive manufacturing, *Green Chem.*, 2023, **25**, 453–466.
5 S.-A. Park, H. Jeon, H. Kim, S.-H. Shin, S. Choy, D. S. Hwang, J. M. Koo, J. Jegal, S. Y. Hwang, J. Park and D. X. Oh, Sustainable and recyclable super engineering thermoplastic from biorenewable monomer, *Nat. Commun.*, 2019, **10**, 2601.
6 J. G. Rosenboom, R. Langer and G. Traverso, Bioplastics for a circular economy, *Nat. Rev. Mater.*, 2022, **7**, 117–137.
7 T. Keijer, V. Bakker and J. Chris Slootweg, Circular chemistry to enable a circular economy, *Nat. Chem.*, 2019, **11**, 190–195.
8 J.-G. Rosenboom, R. Langer and G. Traverso, Bioplastics for a circular economy, *Nat. Rev. Mater.*, 2022, **7**, 117–137.
9 R. A. Sheldon, Green and sustainable manufacture of chemicals from biomass: State of the art, *Green Chem.*, 2014, **16**, 950–963.
10 S. Kamarulzaman, Z. M. Png, E. Q. Lim, I. Z. S. Lim, Z. Li and S. S. Goh, Covalent adaptable networks from renewable resources: Crosslinked polymers for a sustainable future, *Chem*, 2023, **9**, 2771–2816.
11 Z. Wang, M. S. Ganewatta and C. Tang, Sustainable polymers from biomass: Bridging chemistry with materials and processing, *Prog. Polym. Sci.*, 2020, **101**, 101197.
12 F. Della Monica and A. W. Kleij, From terpenes to sustainable and functional polymers, *Polym. Chem.*, 2020, **11**, 5109–5127.
13 C. Wahlen and H. Frey, Anionic Polymerization of Terpene Monomers: New Options for Bio-Based Thermoplastic Elastomers, *Macromolecules*, 2021, **54**, 7323–7336.
14 M. F. M. G. Resul, A. Rehman, A. M. L. Fernández, V. C. Eze and A. P. Harvey, Continuous process for the epoxidation of terpenes using mesoscale oscillatory baffled reactors, *Chem. Eng. Process.*, 2022, **177**, 108998.
15 Y. M. Ahmat, S. Madadi, L. Charbonneau and S. Kaliaguine, Epoxidation of terpenes, *Catalysts*, 2021, **11**, 847.
16 A. Brandolese, D. H. Lamparelli, M. A. Pericàs and A. W. Kleij, Synthesis of Biorenewable Terpene Monomers Using Enzymatic Epoxidation under Heterogeneous Batch and Continuous Flow Conditions, *ACS Sustainable Chem. Eng.*, 2023, **11**, 4885–4893.

 This journal is © The Royal Society of Chemistry 2024

Open Access Article. Published on 24 May 2024. Downloaded on 2/14/2026 11:39:17 PM. This article is licensed under a Creative Commons Attribution-NonCommercial 3.0 Unported Licence.

17 F. Parrino, A. Fidalgo, L. Palmisano, L. M. Ilharco, M. Pagliaro and R. Ciriminna, Polymers of Limonene Oxide and Carbon Dioxide: Polycarbonates of the Solar Economy, *ACS Omega*, 2018, **3**, 4884–4890.

18 O. Hauenstein, S. Agarwal and A. Greiner, Bio-based polycarbonate as synthetic toolbox, *Nat. Commun.*, 2016, **7**, 11862.

19 O. Hauenstein, M. Reiter, S. Agarwal, B. Rieger and A. Greiner, Bio-based polycarbonate from limonene oxide and CO_2 with high molecular weight, excellent thermal resistance, hardness and transparency, *Green Chem.*, 2016, **18**, 760–770.

20 C. Li, R. J. Sablong and C. E. Koning, Synthesis and characterization of fully-biobased α,ω-dihydroxyl poly(limonene carbonate)s and their initial evaluation in coating applications, *Eur. Polym. J.*, 2015, **67**, 449–458.

21 V. B. Moreira, C. Alemán, J. Rintjema, F. Bravo, A. W. Kleij and E. Armelin, A Biosourced Epoxy Resin for Adhesive Thermoset Applications, *ChemSusChem*, 2022, **15**, e202102624.

22 V. Bonamigo Moreira, J. Rintjema, F. Bravo, A. W. Kleij, L. Franco, J. Puiggalí, C. Alemán and E. Armelin, Novel Biobased Epoxy Thermosets and Coatings from Poly(limonene carbonate) Oxide and Synthetic Hardeners, *ACS Sustainable Chem. Eng.*, 2022, **10**, 2708–2719.

23 D. H. Lamparelli, A. Villar-Yanez, L. Dittrich, J. Rintjema, F. Bravo, C. Bo and A. W. Kleij, Bicyclic Guanidine Promoted Mechanistically Divergent Depolymerization and Recycling of a Biobased Polycarbonate, *Angew. Chem., Int. Ed.*, 2023, **62**, e202314659.

24 D. Zhang, E. A. del Rio-Chanona, J. L. Wagner and N. Shah, Life cycle assessments of bio-based sustainable polylimonene carbonate production processes, *Sustainable Prod. Consumption*, 2018, **14**, 152–160.

25 M. Lanzi and A. W. Kleij, Recent advances in the synthesis and polymerization of new CO_2-based cyclic carbonates, *Chin. J. Chem.*, 2024, **42**, 430–443.

26 A. J. Kamphuis, F. Picchioni and P. P. Pescarmona, CO_2-fixation into cyclic and polymeric carbonates: Principles and applications, *Green Chem.*, 2019, **21**, 406–448.

27 S. Paul, Y. Zhu, C. Romain, R. Brooks, P. K. Saini and C. K. William, Ring-opening copolymerization (ROCOP): synthesis and properties of polyesters and polycarbonates, *Chem. Commun.*, 2015, **51**, 6459–6479.

28 S. J. Poland and D. J. Darensbourg, A quest for polycarbonates provided: Via sustainable epoxide/CO_2 copolymerization processes, *Green Chem.*, 2017, **19**, 4990–5011.

29 C. M. Byrne, S. D. Allen, E. B. Lobkovsky and G. W. Coates, Alternating copolymerization of limonene oxide and carbon dioxide, *J. Am. Chem. Soc.*, 2004, **126**, 11404–11405.

30 L. Peña Carrodeguas, J. González-Fabra, F. Castro-Gómez, C. Bo and A. W. Kleij, Al^{III}-Catalysed Formation of Poly(limonene)carbonate: DFT Analysis of the Origin of Stereoregularity, *Chem. – Eur. J.*, 2015, **21**, 6115–6122.

31 N. Kindermann, A. Cristòfol and A. W. Kleij, Access to Biorenewable Polycarbonates with Unusual Glass-Transition Temperature (T_g) Modulation, *ACS Catal.*, 2017, **7**, 3860–3863.

32 T. Stößer, C. Li, J. Unruangsri, P. K. Saini, R. J. Sablong, M. A. R. Meier, C. K. Williams and C. Koning, Bio-derived polymers for coating applications: Comparing poly(limonene carbonate) and poly(cyclohexadiene carbonate), *Polym. Chem.*, 2017, **8**, 6099–6105.

33 C. Martín and A. W. Kleij, Terpolymers Derived from Limonene Oxide and Carbon Dioxide: Access to Cross-Linked Polycarbonates with Improved Thermal Properties, *Macromolecules*, 2016, **49**, 6285–6295.

34 S. Neumann, P. Hu, F. Bretschneider, H. Schmalz and A. Greiner, Blends of Bio-Based Poly(Limonene Carbonate) with Commodity Polymers, *Macromol. Mater. Eng.*, 2021, **306**, 2100090.

35 J. Li, Y. Chen, H. Wu, B. Chen, W. Li, X. Zhu and J. Nie, Enhancement in the Light-Stability of BAPO and ITX-based Photo-Curable Materials via Photobleaching of Pyrrolidene Cyclohexanone, *Prog. Org. Coat.*, 2024, **186**, 108027.

36 B. Steyrer, P. Neubauer, R. Liska and J. Stampfl, Visible Light Photoinitiator for 3D-Printing of Tough Methacrylate Resins, *Materials*, 2007, **10**, 1445.

37 P. Fouassier and J. Lalevée, Three-Component Photoinitiating Systems: Towards Innovative Tailor-Made High-Performance Combinations, *RSC Adv.*, 2012, **2**, 2621–2629.

38 J. Ni, M. Lanzi, D. H. Lamparelli and A. W. Kleij, Ring-Opening Polymerization of Functionalized Aliphatic Bicyclic Carbonates, *Polym. Chem.*, 2023, **14**, 4748–4753.

39 T. M. McGuire, E. M. López-Vidal, G. L. Gregory and A. Buchard, Synthesis of 5- to 8-Membered Cyclic Carbonates from Diols and CO_2: A One-Step, Atmospheric Pressure and Ambient Temperature Procedure, *J. CO_2 Util.*, 2018, **27**, 283–288.

40 I. M. Barszczewska-Rybarek, A. Korytkowska-Wałach, M. Kurcok, G. Chladek and J. Kasperski, DMA Analysis of the Structure of Crosslinked Poly(methyl methacrylate)s, *Acta Bioeng. Biomech.*, 2017, **19**, 47–53.

41 K. P. Menard and N. R. Menard, *Dynamic Mechanical Analysis*, CRC Press, Boca Raton, Florida, 2020.

42 For a recent example see: A. Wambach, S. Agarwal and A. Greiner, Synthesis of Biobased Polycarbonate by Copolymerization of Menth-2-ene Oxide and CO_2 with Exceptional Thermal Stability, *ACS Sustainable Chem. Eng.*, 2020, **8**, 14690–14693.